

USING AIRBORNE ELECTROMAGNETIC SURVEYS TO IDENTIFY POTENTIAL HAZARDS AT COAL WASTE IMPOUNDMENTS: EXAMPLES FROM WEST VIRGINIA¹

Vladislav Kaminski,² Richard W. Hammack, William Harbert, Terry Ackman, James Sams, and
Garret Veloski

Abstract. Mine impoundments have in the past been a cause of catastrophic loss of life and destruction of property. To characterize this potential hazard, helicopter-mounted electromagnetic (HEM) surveys of coal waste impoundments were completed to identify fluid saturated zones within coal waste and to delineate the paths of filtrate fluid flow beneath the decant pond, through the embankment, and into adjacent strata or receiving streams. We also attempted to identify flooded mine workings underlying or spatially adjacent to the waste impoundment areas. In this effort, the National Energy Technology Laboratory of the United States Department of Energy (<http://www.netl.doe.gov>) conducted HEM surveys of 14 coal waste impoundments in southern West Virginia. Five electromagnetic frequencies were used in our surveys (385, 1700, 6536, 28120 and 116300 Hz) and processed using different inversion techniques to determine apparent conductivity depth images (CDI). Follow-up, ground-based resistivity surveys verified the results of the HEM survey. Overall, HEM and ground-based geophysical surveys proved to be effective in delineating the phreatic surface, determining seep locations, locating blockage in engineered drains, imaging areas of unconsolidated slurry, locating areas where process water has invaded adjacent aquifers, potentially depicting the possible location of flooded underground mine workings, locating infiltration zones into the abandoned mines and determining the spatial extent of impoundment impact.

¹ Paper presented at the 7th International Conference on Acid Rock Drainage (ICARD), March 26-30, 2006, St. Louis MO. R.I. Barnhisel Published by the American Society of Mining and Reclamation (ASMR), 3134 Montavesta Road, Lexington, KY 40502
15129

² Vladislav Kaminskiy and William Harbert are Research Associates, National Energy Technology Laboratory, United States Department of Energy, Pittsburgh, PA and a graduate student and Associate Professor respectively at the Dept. of Geology and Planetary Science, Univ of Pittsburgh, PA, USA 15260, Richard Hammack, Terry Ackman, James Sams and Garret Veloski are researchers of the Water and Energy Team, National Energy Technology Laboratory, Pittsburgh, PA, USA 15236-0940.

7th International Conference on Acid Rock Drainage, 2006 pp 902-921

DOI: 10.21000/JASMR06020902

<https://doi.org/10.21000/JASMR06020902>

Introduction

On February 26, 1972, a coal waste impounding structure on Buffalo Creek in West Virginia catastrophically collapsed, releasing approximately 132 million gallons of water (Davies and others, 1972). The resulting flood killed 125 people, injured 1,100, and left more than 4,000 homeless. Factors contributing to the impoundment failure included heavy rainfall and deficiencies in the foundation of the dam, which resulted in the slumping and sliding of the waterlogged refuse bank. This disaster resulted in regulations that governed the design of embankment structures for new impoundments (National Research Council, 2002). Since the implementation of those regulations, no new embankments have failed. However, other types of impoundment failure have occurred, which released water and coal slurry into streams (Table 1). Many of these cases involved the breakthrough of water and coal slurry from impoundments into underground mines. The most notable incident occurred on October 11, 2000 near Inez, Kentucky where 309 million gallons of unconsolidated coal slurry from an impoundment broke into an underground mine and flowed via mine workings into local streams (National Research Council, 2002). Aquatic life was destroyed along miles of stream and temporary shut downs were imposed on a large electric generating plant and numerous municipal water supplies. This incident caused Congress to request the National Research Council to examine ways to reduce the potential for similar accidents in the future. The findings and recommendations of the National Research Council were published in a book titled “Coal Waste Impoundments, Risks, Responses, and Alternatives” (National Research Council, 2002).

In response to the recommendations of the National Research Council, the Robert C. Byrd National Technology Transfer Center (NTTC) at Wheeling Jesuit University in Wheeling, West Virginia contracted Fugro Airborne Surveys to conduct helicopter electromagnetic (HEM) surveys of 14 coal waste impoundments in southern West Virginia (Fig. 1). The surveys were part of a federally funded pilot project to help reduce the dangers of coal slurry impoundments by identifying saturated zones within the coal waste, delineating the paths of filtrate flow beneath the impoundment, through the embankment, and into adjacent strata or receiving streams and identifying flooded mine workings underlying or adjacent to the waste impoundment.

Impoundment failure models

A coal refuse impoundment consists of two major elements: the basin and the embankment (Fig. 2). The basin is underlain by fine-grained coal waste, which is delivered to the upstream side of the embankment via a slurry pipeline and released at a spigot point. The spigot point is moved periodically across the embankment face, thereby creating a series of coalescing, delta-like depositional structures where coarser material accumulates in the vicinity of spigot point and finer material is carried further away. The flooded portion of the basin is sometimes called a “decant pond” because clarified water is returned to the coal cleaning plant for reuse when sedimentation is complete. The basin is bounded on the upstream side by valley walls and on the downstream side by the embankment, which is a dam-like structure that consists of coarse-grained coal waste sometimes mixed with clay or gravel to alter its hydraulic permeability (k). While the impoundment is active, the embankment is constantly being raised to provide more space for coal waste disposal. There are three types of embankment raising: 1) upstream, the most common type for coal waste impoundments; 2) centerline, which is used for true dams; and 3) downstream, which is the most stable structure and is used at sites with high ratios of coarse to

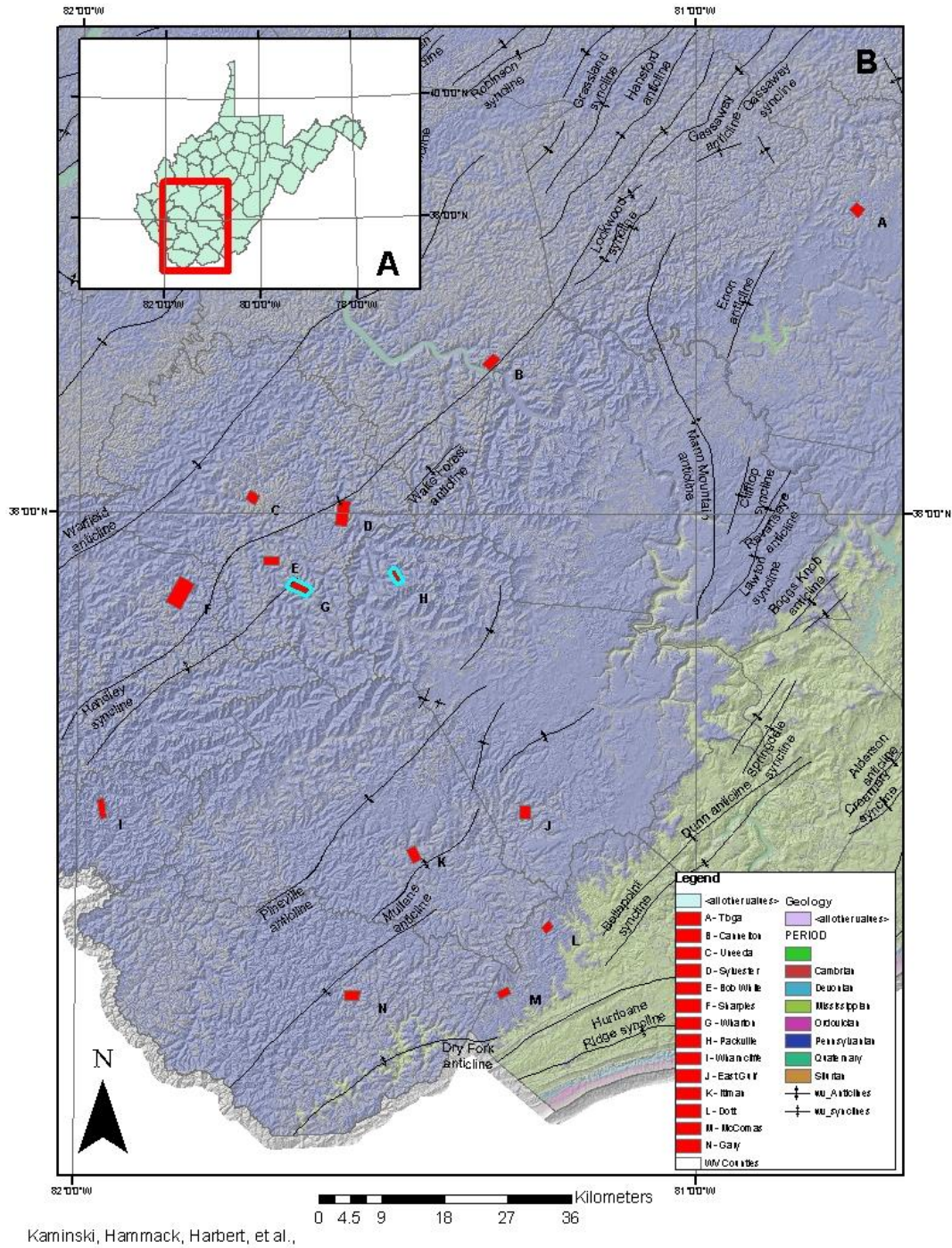


Figure 1. (A) Regional map showing the counties of West Virginia. (B) Higher resolution map showing the location of the HEM surveys. The two sites discussed in detail in this manuscript are outlined.

fine coal waste (Fig. 2). An upstream embankment is raised by placing lifts of coarse material on the top of the embankment and on the fine refuse in the basin near the embankment. The area of the basin where coarse coal waste is mechanically placed over unconsolidated fine coal waste

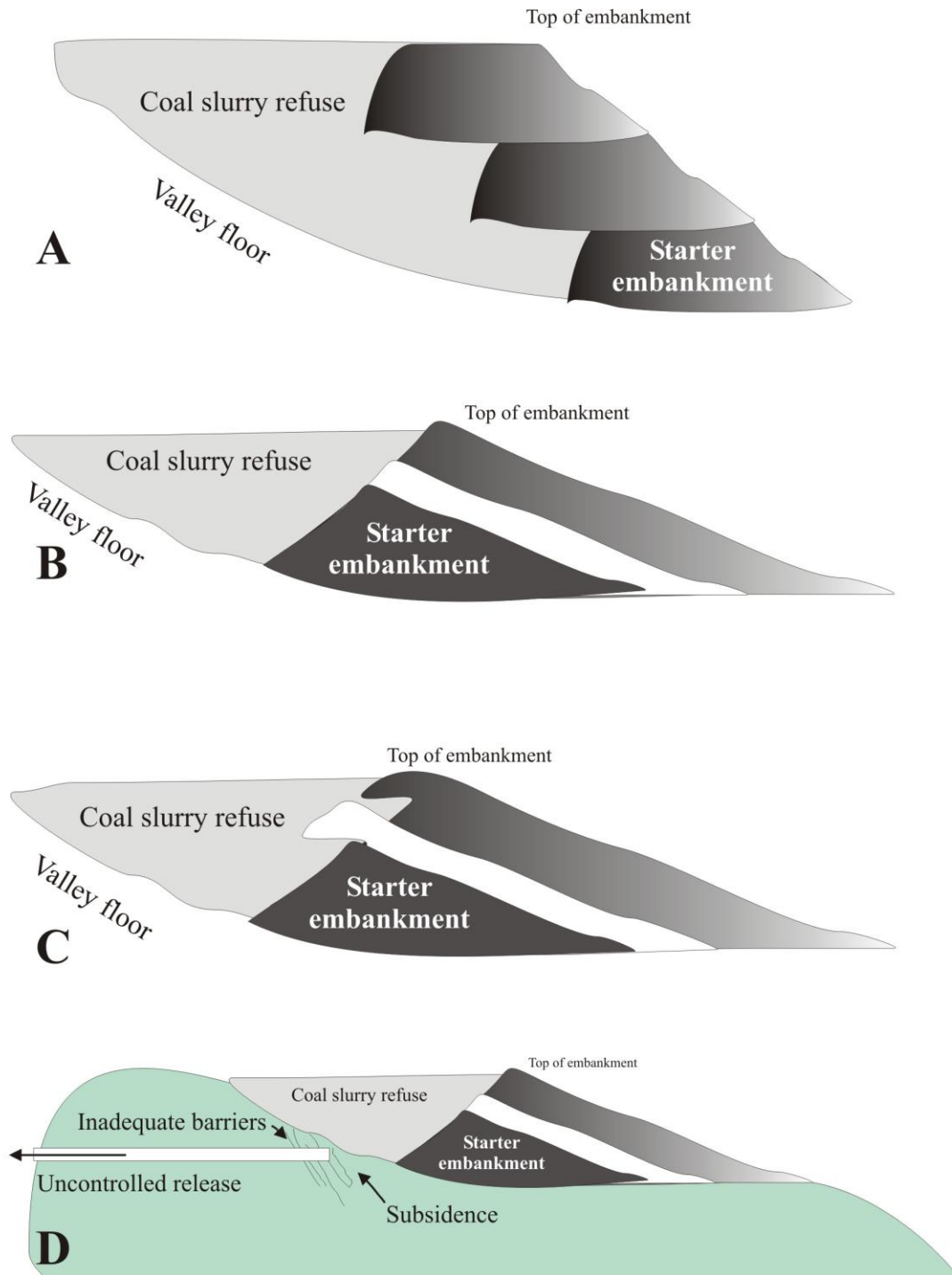


Figure 2. Impoundment types showing (A) Upstream type, (B) Downstream type, (C) Centerline type and (D) possible failure mechanisms related to subsidence and

abandoned underground mine workings. is termed a “push out”. A key factor in embankment stability is the control of internal erosion (piping) and erosion of the downstream face of the embankment. This is done by engineering the embankment so that the hydraulic conductivity increases in a downstream direction, thereby ensuring that any seepage will emerge low on the downstream face of the embankment. Further, many embankments contain surface and subsurface drains to intercept seepage and safely convey it away from the embankment face. The embankment is designed to prevent migration of fines and to minimize water pressure and potential for piping on the downstream side of the embankment (National Research Counsel, 2002). Piping is an underground erosion process, which can occur when there are openings large enough for soil particles to be washed into them and transported with the seeping water. Minimizing piping can be accomplished by the installation of filter and drain zones within the embankment that collect and route water to a downstream toe of the embankment (National Research Counsel, 2002). In addition to the toe drain, there are several other drain types, including chimney drains, finger drains, and blanket drains. Monitoring filtrate propagation through the coarse coal refuse and engineered drains is an important aspect in evaluating safety of an impoundment.

Failure models of a coal slurry impoundment include embankment failure and basin failure. An embankment or basin can each fail in a number of ways. A primary factor differentiating incident cause is the type of embankment construction. Failure causes differ between upstream and downstream types of construction; slope instability and earthquake effects dominate failures of upstream embankments, while foundation failure is more likely to occur in downstream-type embankments.

Overtopping is another cause of impoundment failure, and results when the inflow exceeds the storage capacity of the impoundment. Overflow can occur when the basin is not constructed with sufficient capacity to contain large storm inflow or when engineered spillways are inadequate. Basin failure is most likely to occur in areas where current or past mining is in close proximity to the impoundment. Unfortunately, the location of underground mines is often poorly known due to lack of information (Fig. 2). Factors that must be considered for prevention of basin failure are: subsidence, excessive seepage, and internal erosion. Subsidence disturbs the strata above and adjoining the mining area. It results in the opening of tensile cracks on the surface, displacement along faults and joints, and some distortion of the strata around the working. The immediate roof tends to cave into the working and the floor may heave (National Research Counsel, 2002).

In summary, important factors responsible for impoundment failure include those related to leakage, naturally occurring joints and fractures, overflow, foundation failure, subsidence-induced tension or shear cracks and fractures at the bottom of the decant pond, sinkhole or pit subsidence, piping, or failure related to a catastrophic seismic or storm event. Most of these factors and other possible modes of failure can be identified by electromagnetic geophysical investigations and mitigated.

Survey Description

NTTC selected 14 impoundments for airborne FDEM surveys from a list of impoundments in southern West Virginia that were given a moderate or high hazard potential rating, based on the height of the embankment, the volume of material impounded, and the downstream effects of

an impoundment failure (MSHA, 1974, 1983). Impoundments with moderate hazard potential are in predominately rural areas where failure may damage isolated homes or minor railroads, disrupting services or important facilities. Impoundments with a high hazard potential are those where failure could reasonably be expected to cause loss of human life, serious damage to houses, industrial and commercial buildings, important utilities, highways, and railroads.

The list of selected impoundments was transferred to the National Energy Technology Laboratory where flight areas were determined by constructing a bounding rectangle that enclosed the impoundment and ancillary structures, and included approximately a 1-km wide buffer around the impoundment. The corner coordinates for flight area boundaries were transferred to Fugro Airborne Surveys for final flight planning.

Geophysics Methods

Electro-Magnetic

Noninvasive active geophysical methods used to search for coal mine voids employ artificial, electrical, electromagnetic or mechanical energy to examine the shallow subsurface of the earth (Sharma, 1997; Ward 1990). In contrast, passive geophysical techniques measure some natural physical parameters of the earth, such as variations in earth gravitational or magnetic field. These measurements can be later used to infer stratigraphy, geologic structure, and various other properties of the earth.

Frequency domain electromagnetic (FDEM) methods use a sinusoidal transmitter source tuned to different frequencies to estimate the electrical conductivity of the subsurface. The primary EM field from the transmitter spreads out in space both above and below the ground and induces electrical currents in subsurface conductors, in accordance with the laws of EM induction. These currents give rise to secondary EM fields, which distort the primary field. The secondary or resultant field will differ from the primary field in intensity, phase, and direction (Sharma, 1997), properties that can be measured and used to estimate the conductivity of the subsurface.

Most EM systems employ an active transmitter so that the source geometry and wave frequency can be controlled during field operations. The main function of the artificial field EM methods is the detection of bodies of high electrical conductivity. Electrical conductivity is a function of the electrical properties of the soil and rock matrix. The percentage of fluid saturation and the conductivity of pore fluids determine the electrical conductivity of coal waste materials because electrical current flows through moist or saturated pore spaces in this material and not through the rock fragments themselves. Conductive overburden can shield deeper anomalous zones from detection because near-surface conductors absorb almost all applied energy, thereby preventing deeper penetration.

For coal refuse impoundments, conductive areas were expected to coincide with coal waste material with high water content because of the high conductivity of impoundment fluids. The final product of such survey is a set of Conductivity Depth Images (CDI's), which show the distribution of apparent electrical conductivity in the ground. The CDI's were acquired using 3 different inversion algorithms, EM1DFM, EMFLOW, and EMIGIMA.

Ideally, CDIs showing the vertical distribution of apparent conductivity along flight lines can be used to determine hydrologic conditions beneath the decant pond and within the embankment (Fig. 3). Further, the CDIs may show the location of underground mines if the mines are flooded

with conductive water and are within 50 m of the surface. Limitations such as signal penetration and alternating current (AC) power line interference with the lowest frequency (385 Hz) (Al-Fouzan and others, 2004) can significantly impact the quality of the geophysical signal required to determine the CDI sections.

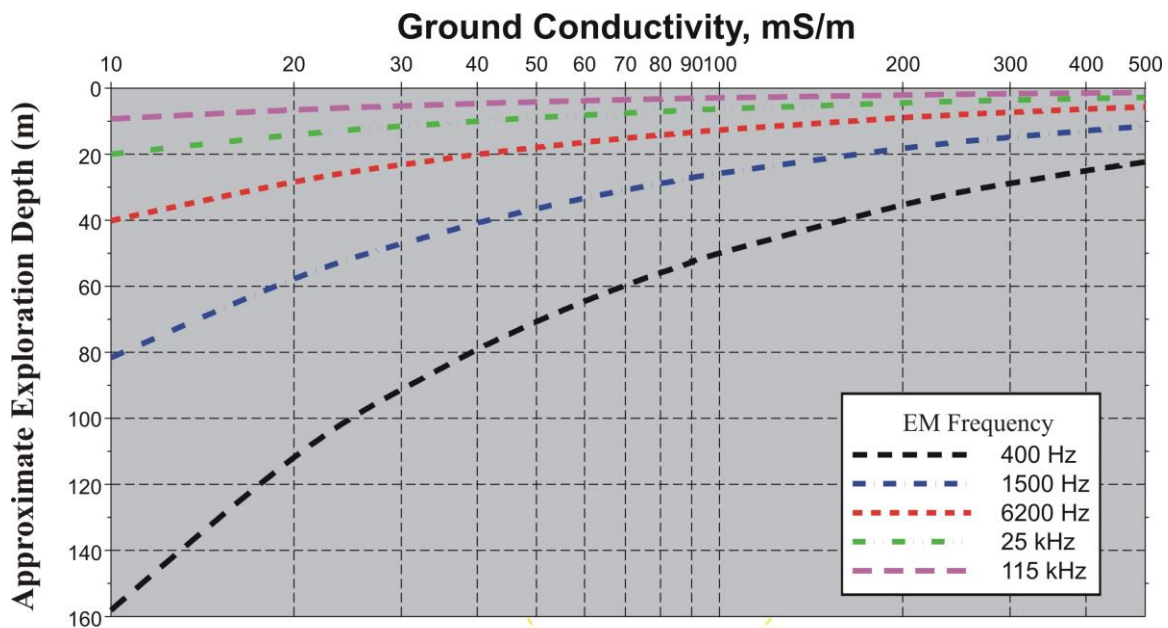


Figure 3. Interpretation palette, describing predicted penetration of EM signal as a function of frequency and earth conductivity. This is a result of solving wave equation derived by combined Ampere's and Faraday's law ($\nabla^2 E + k^2 E = 0$ and $\nabla^2 H + k^2 H = 0$). The solution of the wave equation is $E = E_0 e^{-ikz}$, $H = H_0 e^{-ikz}$, where E and H are electrical and magnetic fields, z is the penetration depth and k is the wave number equal to $\sqrt{-i\omega\mu\sigma}$, where ω – is the electromagnetic survey frequency and σ – is the earth conductivity. Note that earth conductivity strong influences the penetration depth of the electromagnetic signal.

DC resistivity profiling

DC resistivity profiling was used on the ground to corroborate helicopter results. DC resistivity profiling uses an array of electrodes (stainless steel stakes driven into the ground) deployed at regular intervals along a line. For this study, current was injected into the ground via current electrodes and potentials were measured between as many as eight pairs of potential electrodes for each current injection. The current injection and potential electrode polling was conducted using a dipole dipole array. The geometry of current flow is such that wider electrode spacing results in deeper current penetration. This method can be used to produce an apparent resistivity depth section along the profile. Because resistivity is the inverse of conductivity, this information, which is obtained from ground measurements, can be used to verify helicopter results.

Geophysical Survey and Processing

In July 2003, Fugro Airborne Surveys performed frequency domain electromagnetic (FDEM) surveys of the selected coal refuse impoundments using the RESOLVE electromagnetic data acquisition system. This system consists of five coplanar transmitter/receiver coil pairs operating at frequencies of 385, 1700, 6536, 28120 and 116300 Hz and one coaxial transmitter/receiver coil pair that operated at a frequency of 1.41 kHz. Separation for the five coplanar coil pairs was 7.9 m; separation for the coaxial coils was 9 m (a complete description of the RESOLVE data acquisition system is available at <http://www.fugroairborne.com/>). An optically pumped cesium vapor magnetometer mounted within the RESOLVE sensor was used to acquire total field magnetic data concurrent with the collection of electromagnetic data.

The surveys were flown using an Ecureuil AS350-B2 helicopter with the RESOLVE sensor suspended about 30 m beneath the helicopter as a sling load. Survey information was acquired by flying parallel lines approximately 50 m apart while attempting to maintain the sensor at an altitude of 35 m. However, the average sensor height during these surveys was 45 m because the rugged terrain, trees, and numerous power lines necessitated higher flight in certain areas for safety. At a nominal flight speed of 90 km/hr, the 10 Hz data acquisition rate resulted in one reading every 2.5 meters along the flight line.

Preliminary data processing including leveling and digital filtering was performed by Fugro Airborne Surveys. Electronic data were then transferred to NETL for additional processing, analysis, and interpretation. These data included conductivity maps for five frequencies and a CSV text file containing leveled in-phase, quadrature, and navigational data.

At the United States Department of Energy National Energy Technology Laboratory in Pittsburgh, conductivity and total magnetic field intensity maps were incorporated into geographical information system (GIS) project based geodatabases, which were constructed for each site. Within the GIS environment, the locations of conductivity anomalies can be related to specific attributes of the coal refuse impoundment as well as the locations of known underground mine workings. In-phase and quadrature data were used to construct conductivity/depth images (CDI) and Sengpiel sections using EM1DFM, EMFlow and EMIGMA. CDI sections and Sengpiel sections were related to features on maps and air photos using custom viewing software developed at NETL (Veloski and Lynn, 2005).

The HEM data were initially processed using three software codes to generate CDIs. These codes included EM1DFM, developed at the University of British Columbia (UBC), EMFlow, a commercial code marketed by Encom, an Australian company, and EMIGMA developed and marketed by Petrov Eikon, a Canadian company. CDIs from each of the three softwares were evaluated; only CDIs from EM1DFM were used in final interpretations because this software provided the most geologically reasonable interpretation.

EM1DFM software was used to generate conductivity/depth images for each line of the HEM survey including the three tie lines. The CDIs have conductivities ranging from 0 to 200 mS/m and are indicated with a color ramp of blue (resistive) to red (conductive). We interpret the sharp change in conductivity with depth to denote the boundary between the unsaturated zone (resistive, blue) and saturated zone or water table (conductive, yellow-red). The upper 100 m of the CDI is used for interpretation; conductors below this depth are assumed to be an artifact of the processing or noise due to power lines.

Upon the completion of the HEM survey and geophysical processing, two impoundments were selected for more detailed study. In the summer of 2005, field surveys were conducted at the Jarrell's Branch and Brushy Fork Slurry impoundments to verify the HEM results. Ground surveys were completed using the 56 electrode SuperSting resistivity system in source-receiver dipole-dipole geometry.

Interpretation

The primary goal of this study was to evaluate HEM as a means to quickly screen coal waste impoundments and look for indicators of potential failure. HEM was expected to be a good tool for determining hydrologic conditions within the impoundments because of the contrast in electrical conductivity between: 1) coal waste and bedrock, 2) unsaturated and seepage-saturated coarse coal waste, 3) consolidated and unconsolidated fine coal waste, and 3) flooded underground mines and bedrock. Certain hydrologic conditions are undesirable in impoundments and can be recognized in CDIs generated from HEM survey data.

Control of Phreatic Surface

The phreatic surface is defined as the top of the zone of saturation or water table, which is open to atmospheric pressure. Within coal waste impoundments, it is desirable that the phreatic surface emerge near the toe of the downstream embankment to prevent piping and surface erosion. Figure 4 illustrates the desired phreatic surface through an embankment. A CDI profile collected across a normal impoundment is shown in Fig. 5. The CDI shows conductors (yellow-red) that represents unconsolidated fine-grained slurry in the basin and filtrate flow through the embankment, emerging near the base of the downstream slope. The resistive surface layer in the basin is a push out of coarse coal refuse. Most impoundments exhibited normal filtrate seepage through the embankment with the phreatic surface emerging near the impoundment base.

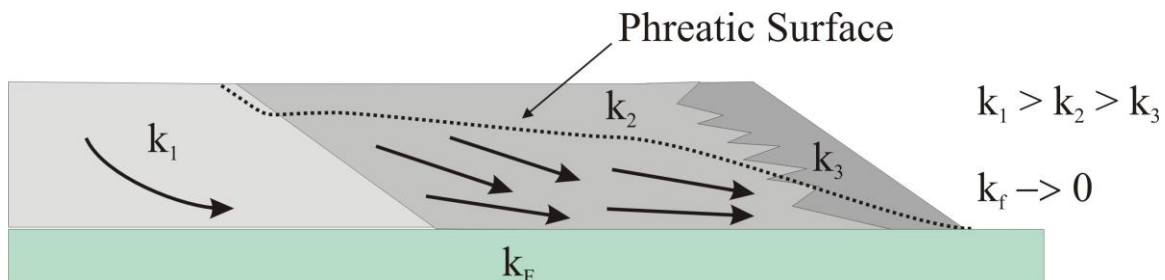


Figure 4. Geometry of phreatic surface within the tailings impoundment. In this figure, the variable k corresponds is the hydraulic conductivity; specific hydraulic conductivity coefficients: k_1 – hydraulic conductivity of the embankment, comprised of coarse coal refuse material mixed with clay, k_2 – hydraulic conductivity of the intermediate zone, k_3 – hydraulic conductivity of consolidated coal slurry close to the spigot point and k_f – hydraulic conductivity of the bedrock.

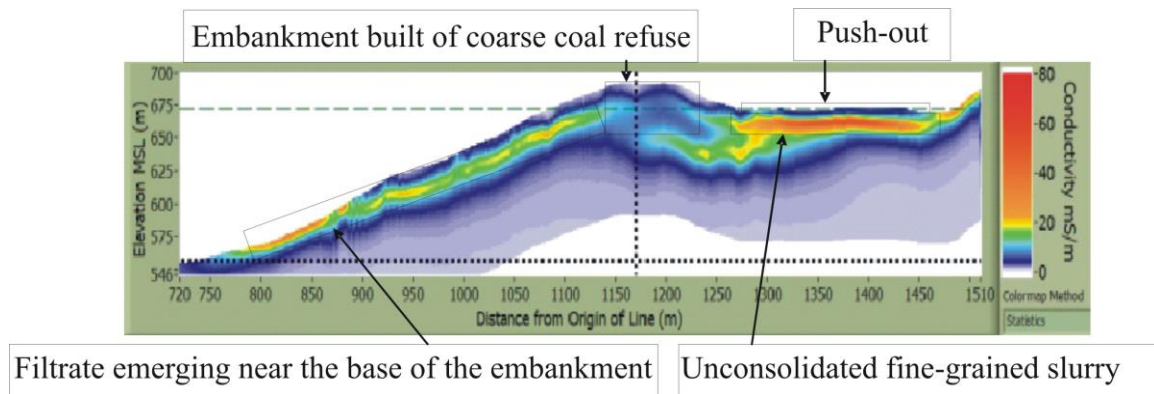
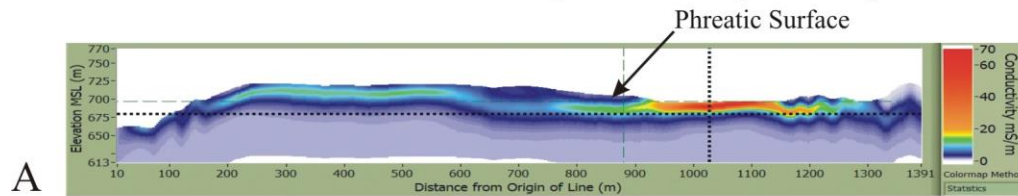


Figure 5. Interpretation of a CDI HEM-derived apparent conductivity cross-section, showing toe-type drain of an upstream-type impoundment. Elevation and distance along the profile are in meters, the scale of apparent conductivity in units of mS/m is shown on the right hand portion of the figure. Four impoundment related elements are shown: The push-out, which is newly emplaced coarse-grained refuse, characterized by lower electrical conductivity values, unconsolidated fine-grained refuse mixed with water, which is the conductive material underneath the push-out, the dam structure, which is comprised of coarse-grained refuse mixed with clay and characterized by low conductivity values and the filtrate flow underneath the dam, emerging at the toe (base) of the dam. Note that each element has a clear geophysical signature with respect to the HEM.

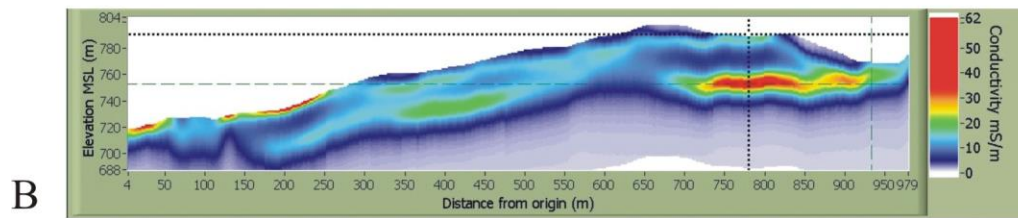
Interpretation of HEM derived CDIs from different impoundments allowed us to observe the effect of a changing spigot point location on the distribution of unconsolidated coal slurry in the basin (Fig. 6). One example where decant pond waters invaded adjacent aquifers was identified (Fig. 6). Because of its susceptibility to seismic events, unconsolidated coal slurry located underneath the embankment (Fig. 6) is of particular concern. Bodies of unconsolidated coal refuse are easily discerned in CDIs because unconsolidated coal slurry is much more conductive than coarse coal waste.

Brushy Fork and Jarrell's Branch Impoundments are examples of an upstream and a downstream raised embankment, respectively. The hydrologic environments that have developed within the embankments of these two impoundments are very different. Figure 7A is a CDI from a flight line at the Jarrell's Branch Impoundment. This design facilitates the incorporation of drains into the downstream embankment, particularly blanket drains. In Fig. 7A, two conductors can be seen within the downstream embankments that are interpreted to be filtrate flow paths. Filtrate flowing within the upper flow path emerges at the base of terraces where toe drains transport it to trenches along either abutment. Filtrate flowing in the lower flow path does not emerge until it reaches the base of the embankment. Figure 7B is a CDI from a flight line across the Brushy Fork Impoundment, an upstream raised impoundment. By the nature of its construction, it is more difficult to incorporate subsurface drains into the downstream slope of this type of impoundment. Only one filtrate flow path is noted and it emerges at the surface at numerous locations along the downstream slope of the embankment.

Invasion of waters from decant pond into adjacent aquifers



Unconsolidated slurry underneath the embankment



Effect of changing spigot point location

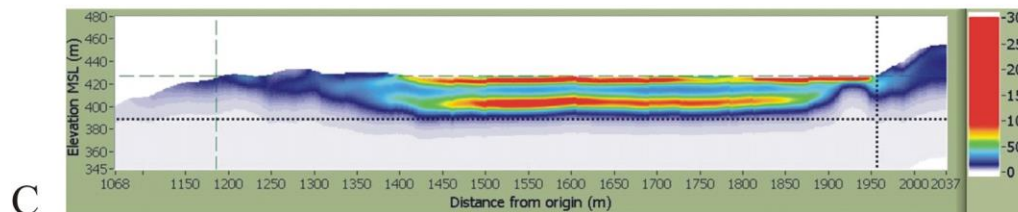


Figure 6. The cross-section is made along one of the flight lines and perpendicular to the pond-embankment direction. The phreatic surface of the filtrate is clearly defined as a conductive contour, following the terrain at 5 to 10 meter depth. (A) This CDI section shows the invasion of waters from decant pond into adjacent aquifers. (B) This CDI shows what we interpret to be a thick plume of unconsolidated slurry underneath the embankment. Potentially this may raise concern regarding the dam stability. (C) This CDI shows a variation in apparent conductivity, which we believe suggests a spigot point change. Spigot point creates delta-like structures with coarser material deposited closer to withdrawal location and finer - deposited further away. In case of slurry, deposited into the pool - coarser material is more conductive, so changing the spigot point from one side of the pool to another (as commonly practiced in coal industry) can create a structure which is layered in terms of electrical conductivity, similar to what is observed on the figure.

Figure 8 shows an interpreted CDI, which could show a flooded underground mine working at the Monclo impoundment. Additional ground-based geophysical investigations are being undertaken to investigate this region.

Ground resistivity surveys were conducted in 2005 across two recent push outs at Jarrell's Branch and Brushy Fork Impoundments. The resistivity ground survey (Fig. 9) conducted across a push out at Jarrell's Branch Impoundment found a resistive surface layer (coarse coal waste) overlying a more conductive layer (unconsolidated fine coal waste). Resistive bedrock is visible at the base of the section. The ground survey results verified the HEM observations when one

considers that the push out has moved upstream between the 2003 HEM survey and the 2005 resistivity survey.

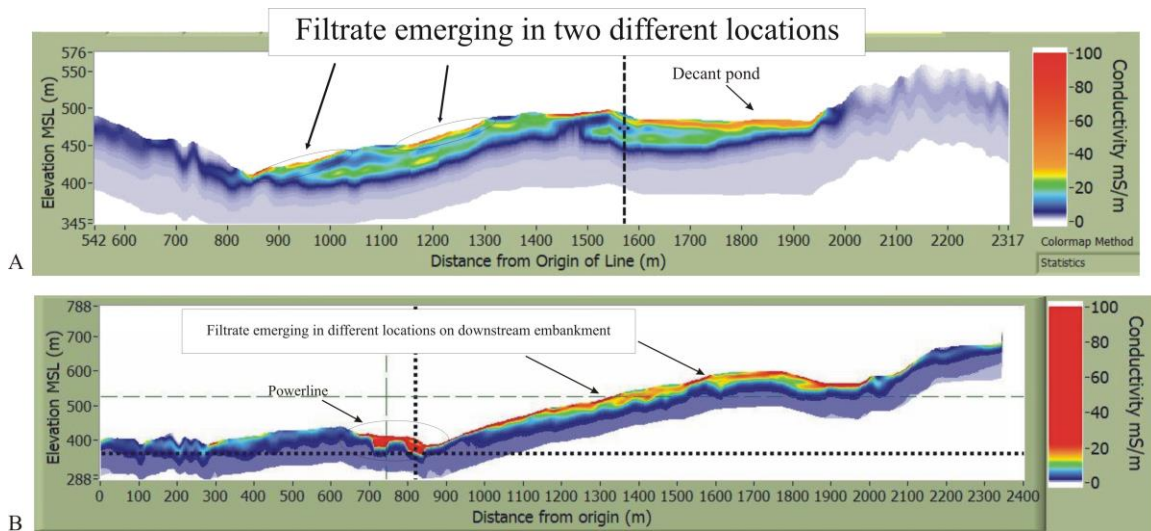


Figure 7. (A) CDI from the Jarrell's Branch impoundment, which shows a blanket drain within a downstream-type impoundment emerging at two different locations along the slope of the dam. (B) CDI from the Brushy Fork impoundment, which shows filtrate drain emerging in different locations throughout the length of the dam slope.

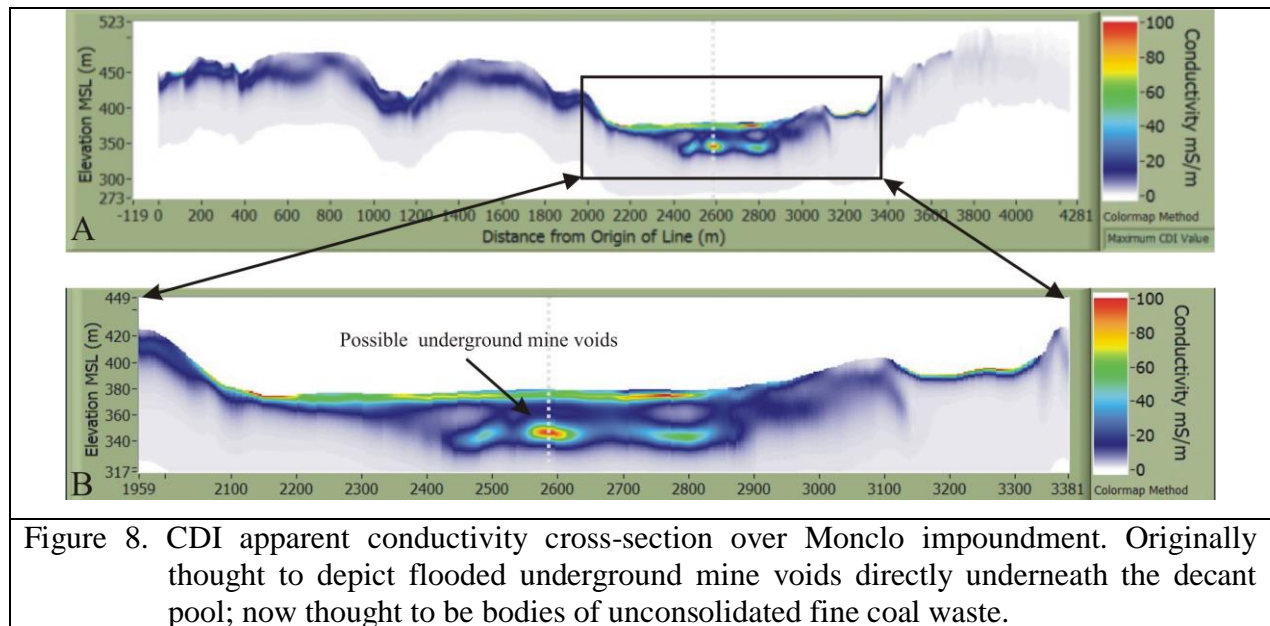


Figure 8. CDI apparent conductivity cross-section over Monclo impoundment. Originally thought to depict flooded underground mine voids directly underneath the decant pool; now thought to be bodies of unconsolidated fine coal waste.

Although a well defined bedrock basement signature was observed at Jarrell's Branch Impoundment (Fig. 9) there is no evidence of bedrock at Brushy Fork Impoundment even to a

depth of about 50 m in the airborne or field survey (Fig. 10). However, there is a deep resistive area at about 150 m along the section (Fig. 10D) that could be interpreted as a bedrock ridge.

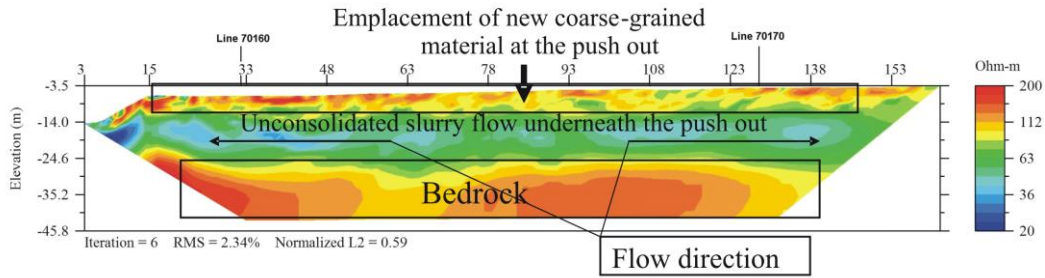


Figure 9. An apparent conductivity cross-section, acquired during a field survey using the Supersting resistivity system data at the Jarrell's Branch impoundment push-out.

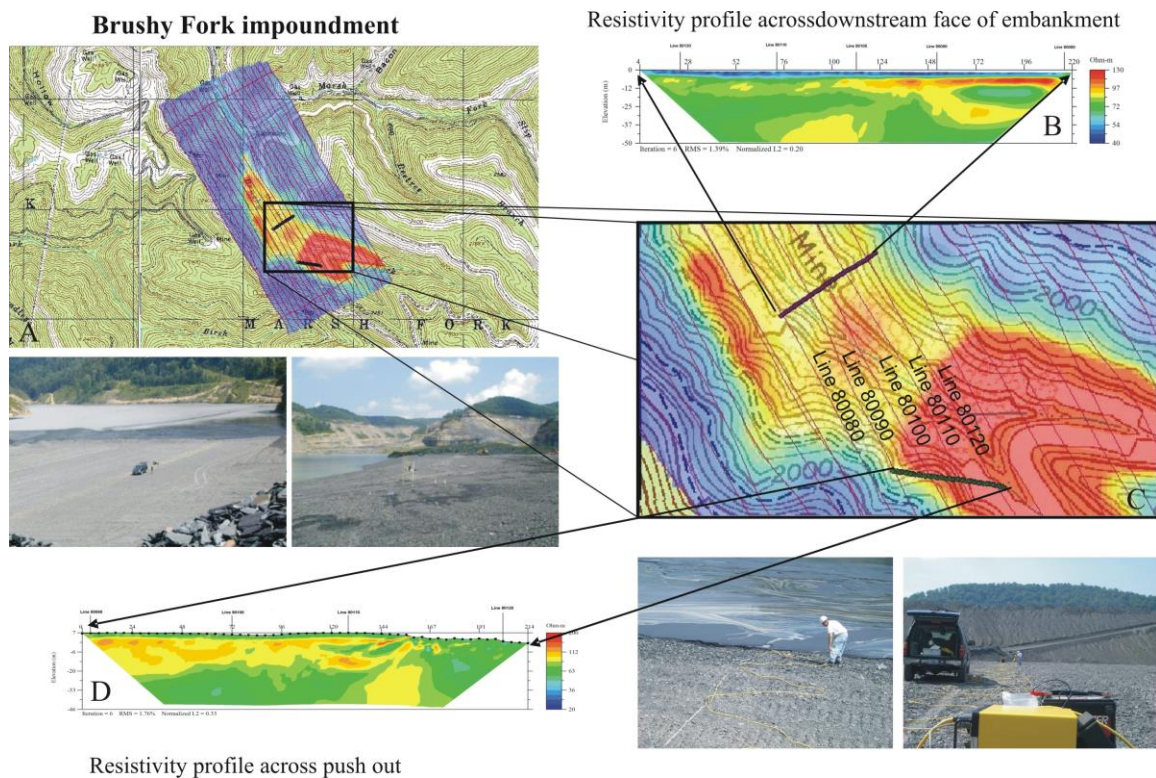


Figure 10. Combination of ground-based (Supersting Resistivity) and airborne (Fugro-Resolve) geophysical techniques implemented to analyze the push-out and the dam at Brushy Fork Impoundment. (A) An HEM derived apparent conductivity map collected at the 116300 Hz frequency and laid over a digital raster graphic. (B) CDI cross-section showing the apparent resistivity collected at the dam. (C) The field survey profiles were laid across five HEM flight-lines in this higher resolution map of the 116300 Hz HEM derived apparent conductivity. (D) CDI cross-section of the apparent resistivity data collected at the push-out, with the profile laid across four HEM flight-lines (80090, 80100, 80110 and 80120). Upper right figure depicts a conductivity map gridded from airborne conductivity data, collected at 116 KHz frequency and laid over a digital raster graphic. Field photographs were taken at the Brushy Fork impoundment.

At Brushy Fork Impoundment, the coarse coal refuse placed on the surface of the push out is more conductive than the surface layer at Jarrell's Branch Impoundment. This difference can be attributed to the Brushy Fork Impoundment material being moister and more clayey than that the coarse refuse at Jarrell's Branch Impoundment.

Some components appeared to deliver sufficient electrical contrast to adequately delineate them throughout the entire survey region entirely based on geophysical data, some had to be interpreted basing the judgment on supplementary information such as elevation, slope, hydrological data, impoundment construction and surface maps, acquired from mining companies.

HEM data from the 14 impoundments were examined to identify flooded mines beneath or adjacent to the decant pond. It was thought that a mine flooded with conductive water might be detected by HEM when surrounded by resistive strata. One site, the Monclo impoundment, appeared to contain such an underground feature on the basis of interpretation of the subsurface HEM derived apparent conductivities. In Fig. 10, a CDI section shows conductive underground anomalies underneath the decant pond, which were originally thought to indicate the presence of flooded workings. However, engineers familiar with the impoundment say that there are no mine workings at the elevation of the conductive anomalies. Rather, the anomalies are within the fine coal waste that has been placed in the basin and probably represent areas of unconsolidated slurry. Currently the Monclo impoundment is being investigated with further ground-based geophysical surveys including reflection/refraction seismic and resistivity surveys planned for the next field season.

Ground survey interpretation

Visually, the push-out at the Brushy Fork Impoundment was similar to a push-out at the Jarrell's Branch Impoundment that was surveyed on June 23, 2005. Both show a resistive layer (coarse coal waste) overlying a conductive layer (unconsolidated fine coal waste). However, the resistivity profiles show that the two push-outs differ in the resistivity of the coarse coal waste. The Brushy Fork Impoundment survey depicted push-out material that was less resistive (more conductive) than the material comprising the Jarrell's Branch Impoundment push-out. The moisture content for the coarse coal waste is about 10% at this site, which is typical. Therefore, the difference in resistivity could be due to differences in clay content (higher clay content results in lower resistivity). This will have to be confirmed in future.

Further, the resistivity profile from Jarrell's Branch Impoundment showed a conductive layer (interpreted to be unconsolidated coal slurry) encapsulated between two resistive layers (the upper interpreted to be coarse coal waste; the lower interpreted to be bedrock). However, the Brushy Fork Impoundment resistivity profile showed only a thin, discontinuous resistive layer overlying a relatively uniform and more conductive material. The rapid placement of coarse refuse at Brushy Fork Impoundment (350,000 tons/month) could have been responsible for displacing rather than encapsulating the fine coal refuse. In such a case, there would be no fine coal refuse remaining to give rise to a conductive layer in the resistivity profile. No bedrock can be discerned in the Brushy Fork Impoundment resistivity profile because the depth to bedrock at this location is 115 m, which is well below the 50-m exploration depth for the resistivity survey (Paul McCombs, personal communication).

Conclusions

Airborne electromagnetic and ground-based geophysical surveys have been shown to be effective in delineating the phreatic surface, determining seep locations, locating blockage in engineered drains, imaging areas of unconsolidated slurry, locating areas where process water has invaded adjacent aquifers, constraining the possible location of flooded underground mine workings, locating infiltration zones into the abandoned mines and determining the spatial extent of impoundment impact.

Acknowledgements

The reviewers of this manuscript and volume editor are gratefully acknowledged for their help in considerably improving this manuscript. The review of a preliminary version of this manuscript by Dr. Robert L. Kleinmann was very helpful. Discussions in the field with Mr. Paul McCombs were very useful in understanding details of the Bushy Fork impoundment. This work was partially funded with support from NETL/DOE award 12.

References

- Akima, H., 1978, A method for bivariate interpolation and smooth surface fitting for irregularly distributed data points: ACM Transactions on Mathematical Software, 4, p. 148-159. <http://dx.doi.org/10.1145/355780.355786>.
- Al-Fouzan, F., Harbert, W., Dilmore, R., Hammack, R., Veloski, G., and Ackman, T., 2004, Methods for Removing Signal Noise from Helicopter Electromagnetic Survey Data, Mine Water and the Environment, v. 23, p. 28-33. <http://dx.doi.org/10.1007/s10230-004-0033-3>.
- Cooper, B.N., 1944, Geology and Mineral resources of the Burkes Garden quadrangle, Virginia: Virginia Geological Survey Bulletin 60, p. 229.
- Custis, K., 1994, Application of geophysics to acid mine drainage investigations, Volume 1 - Literature review and theoretical background: California Department of Conservation, Office of Mine Reclamation.
- Davies, W.E., Bailey, J.F., and Kelly, D.B., 1972, West Virginia's Buffalo Creek flood - a study of the hydrology and engineering geology: U.S. Geological Survey Circular 667, p. 32.
- Domenico, P. A., and F. W. Schwartz, 1998, Physical and chemical hydrogeology: Second Edition, New York, John Wiley & Sons.
- Edmunds, W. E., V. W. Skema, and N. K. Flint, 1999, Stratigraphic and sedimentary tectonics, in Shultz, C., ed., The Geology of Pennsylvania, Pennsylvania Geological Survey & Pittsburgh Geological Society, Special Publication 1, p.149-169.
- Encom, 2001, EM Flow electromagnetic data display, analysis and interpretation: Encom Technology Pty. Ltd.
- Englund and others, 1968, Geologic map of the Bramwell quadrangle, West Virginia: U.S. Geological Survey Geologic quadrangle map GQ-745, scale 1:24,000.
- Englund, K.J., Arndt, H.H., and Henry T.W., (eds), 1979, Proposed Pennsylvanian System Stratotype, Virginia and West Virginia (Ninth International Congress of Carboniferous

- Stratigraphy and Geology meeting guide and geology meeting Guidebook Field Trip D): Washington, D.C., American Geological Institute, p. 136.
- EPA Region 3, 1994, Streams impacted by acidic drainage from coal mines in EPA Region 3: U.S. Environmental Protection Agency, http://www.epa.gov/nsdi/projects/r3_mines.html.
- Fraser, D.C., 1978, Resistivity mapping with an airborne multicoil electromagnetic system: *Geophysics*, 43, p. 144-172. <http://dx.doi.org/10.1190/1.14408172>.
- Fugro Airborne Surveys, 2002, Logistics report helicopter-borne resolve electromagnetic and magnetic geophysical survey Kettle Creek, Pennsylvania: Fugro Airborne Surveys, Inc.
- Kearey, P. and Brooks, M., 1991, *An Introduction to Geophysical Exploration*, Second Edition, Oxford, Blackwell Scientific.
- Kleinmann R. L. P, 1989, Acid mine drainage: U.S. Bureau of Mines researches and develops control methods for both coal and metal mines: *Engineering and Mining Journal*, 19, 16I-16N.
- Macnae, J.C., A. King, N. Stolz, A. Oxmakoff, A. Blaha, 1998, Fast AEM data processing and inversion: *Expl. Geophys.*, *Austr. Soc. Expl. Geophys.*, 29, 163-169. <http://dx.doi.org/10.1071/EG998163>.
- Manahan, S. E., 2000, *Environmental chemistry*, 7th Edition: CRC Press.
- MSHA [Mine Safety and Health Administration] 1974. Design guidelines for Coal Refuse Piles and Water, Sediment or Slurry Impoundments and Impounding Structures. Informational Report 1109. U.S. Department of Labor, p. 29.
- MSHA. 1983. Design guidelines for Coal Refuse Piles and Water, Sediment or Slurry Impoundments and Impounding Structures. Informational Report 1109. U.S. Department of Labor, p. 29.
- National Research Council, 2002, *Coal Waste Impoundments Risks, Responses, and Alternatives*, National Academy Press, Washington D.C.
- Reger D.B., 1926, Mercer, Monroe and Summers Counties: West Virginia Geological Survey [county report], p. 963.
- "Reynolds, J. M., 1997, *An Introduction to Applied and Environmental Geophysics*, John Wiley and Sons, New York.
- Sams, J. I., and G. A. Veloski, 2003, Evaluation of airborne thermal infrared imagery for locating mine drainage sites in the Lower Youghiogheny River Basin, Pennsylvania, USA: *Mine Water and Environment*, 22, p. 85-93. <http://dx.doi.org/10.1007/s10230-003-0005-z>.
- Sengpiel, K. P., 1988, Approximate inversion of airborne EM data from a multilayered ground; *Geophy. Pros.*, 36, p. 446-459. <http://dx.doi.org/10.1111/j.1365-2478.1988.tb02173.x>.
- Sharma, P. V., 1986, *Geophysical Methods in Geology*, Second Edition, Elsevier Science, New York.
- Sissler, J. D., 1924, Bituminous coal losses and mining methods in Pennsylvania including thickness, character and reserves of coal, topographic and geologic survey: Commonwealth of Pennsylvania Department of Forests and Waters, United States Coal Fact Finding Commission and United States Bureau of Mines.

Stumm, W., and J. J. Morgan, 1981, Aquatic chemistry: John Wiley & Sons.

Telford, W.M., Geldart, L.P., and Sheriff, R. E., 1990, Applied Geophysics Second Edition, Cambridge University Press, Cambridge UK.
<http://dx.doi.org/10.1017/CBO9781139167932>.

Ward, S.H. 1990. Geotechnical and Environmental Geophysics, vol 1-3. Tulsa, OK: Society of Exploration Geophysics <http://dx.doi.org/10.1190/1.9781560802785>

Table 1. Listing of Coal Impoundment Spills from <http://www.coalimpoundment.org/spill/spillList.asp>

Year	Spill Volume (Gallons)	Company	Town	County	State	River System
1972	132,000,000	Pittston Coal Company	Lorado	Logan	WV	Guyandotte River
1977	2,200,000	Island Creek Coal Company	Bob White	Boone	WV	Little Coal River
1980	168,000	Philpot Coal Corp.		Raleigh	WV	
1980		Unknown		Mercer	WV	
1981		Belva Coal Co.	Earling	Logan	WV	Guyandotte
1981	25,000,000	Eastover Mining Company	Ages	Harlan	KY	Cumberland River
1987	7,500,000	Unknown		Floyd	KY	
1987	23,000,000	Peabody Coal Company	Montcoal	Raleigh	WV	Coal River
1988	6,500,000	Tennessee Consolidated Coal Co.	Whitwell	Marion	TN	Tennessee River
1991	10,000,000	Great Western Coal, Inc.	Coalgood	Harlan	KY	Cumberland River
1994	375,000	Consolidation Coal Company	Granville	Monongalia	WV	Monongahela River
1994	112,000,000	Massey Energy Company	Inez	Martin	KY	Big Sandy River
1994	14,000,000	Cumberland Coal Company		Harlan	KY	
1995		Lady H Coal Co.	Green Valley	Nicholas	WV	Gauley River
1995	1,200,000	Consolidation Coal Company	Oakwood	Buchanan	VA	Big Sandy River
1996	1,000,000	Arch Coal, Inc.	St. Charles	Lee	VA	Powell River
1996	6,000,000	Arch Coal, Inc.	St. Charles	Lee	VA	Powell River
1996	4,000,000	Consolidation Coal Company	Oakwood	Buchanan	VA	Big Sandy River
1997	1,000	Ashland Coal	Julian	Boone	WV	Little Coal River

1997	1,000,000	Ashland Coal		Julian	Boone	WV	Little River Coal
1999		Massey Energy Company		Sundial	Raleigh	WV	Coal River
1999	1,500	Massey Energy Company		Sylvester	Boone	WV	Coal River
1999	2,200	Massey Energy Company		Sylvester	Boone	WV	Coal River
2000	309,000,000	Massey Energy Company		Inez	Martin	KY	Big Sandy River
2001	1,000,000	Premier Coal Co.	Elkhorn	Jenkins	Letcher	KY	
2001	30,000	Massey Energy Company		Uneeda	Boone	WV	Little River Coal
2001		Massey Energy Company		Quinland	Boone	WV	Little River Coal
2001	50,000	Massey Energy Company		Dehue	Logan	WV	Guyandotte River
2001	15,000	Massey Energy Company		Madison	Boone	WV	Little River Coal
2001		Massey Energy Company		Quinland	Boone	WV	Little River Coal
2001		Massey Energy Company		South Williamson	Pike	KY	Big Sandy River
2001	4,000	Massey Energy Company		Sidney	Pike	KY	Big Sandy River
2002		Massey Energy Company		Quinland	Boone	WV	Little River Coal
2002	135,000	Massey Energy Company		Sidney	Pike	KY	Big Sandy River
2002	10,000,000	Abandoned Mine Land		Wilcoe	McDowell	WV	Big Sandy River
2002	25,000	Arch Coal		Julian	Boone	WV	Little River Coal
2002	20,000	Massey Energy Company		Delbarton	Mingo	WV	Big Sandy River
2002	100,000	Massey Energy Company		Dehue	Logan	WV	Guyandotte River
2002		James River Coal Company		Slemp	Perry	KY	Kentucky River

2003	1,000	Massey Energy Company	Summersville	Nicholas	WV	Gauley River
2003		Massey Energy Company	Uneeda	Boone	WV	Little Coal River
2003		Abandoned Mine Land	Sprattsville	Mingo	WV	Guyandotte River
2003	20,000	Massey Energy Company	Sidney	Pike	KY	Big Sandy River
2003	27,000	Massey Energy Company	Dehue	Logan	WV	Guyandotte River
2003		Falcon Land Co.	Omar	Logan	WV	Guyandotte River
2003		Falcon Land Co.	Omar	Logan	WV	Guyandotte River
2003		James River Coal Company	Slemp	Perry	KY	Kentucky River
2003	250,000	Massey Energy Company	Prenter	Boone	WV	Big Coal River
2003	250,000	Massey Energy Company	Uneeda	Boone	WV	Little Coal River
2003		White Mountain Mining Co., L.L.C.	Rhodell	Raleigh	WV	Guyandotte River
2003		Rapoca Group	Big Rock	Buchanan	VA	Big Sandy River
2003	1,000	Island Creek Coal Co.	Oakwood	Buchanan	VA	Big Sandy River
2004		Massey Energy Company	Dehue	Logan	WV	Guyandotte